

Rapid Naked-Eye Detection of a Liver Disease Biomarker by Discovering Its Monoclonal Antibody to Functionalize Engineered Red-Colored Bacteria Probes

Ding Shen,^{||} Wei Hu,^{||} Suqing Zhao,* and Chuanbin Mao*Cite This: *ACS Omega* 2021, 6, 32005–32010

Read Online

ACCESS |



Metrics & More



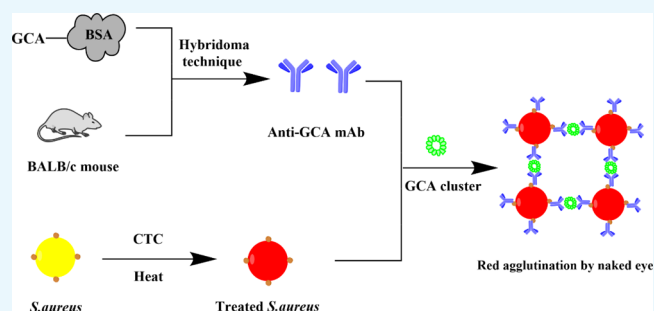
Article Recommendations



Supporting Information

ABSTRACT: Glycocholic acid (GCA) is a biomarker for liver diseases, but few facile naked-eye detection methods have been reported to detect it till now. To tackle this challenge, we first prepared a novel monoclonal mouse antibody (mAb) of GCA by a hybridoma technique. The anti-GCA mAb exhibited high specificity, making its cross-reactivity with seven structurally and functionally related GCA analogs negligible. Using this anti-GCA mAb and an engineered red-colored bacterial strain (*Staphylococcus aureus*, *S. aureus*), we developed a simple naked-eye visualized method for GCA detection. Toward this goal, *S. aureus* bacteria were turned red by 5-cyano-2,3-ditolyl tetrazolium chloride

treatment and heat treated to an unculturable state, rendering the bacteria as an optical detection probe powerful in *in vitro* diagnostics. Through the natural binding ability of protein A on the surface of *S. aureus* and the Fc fragment of a mouse antibody, the anti-GCA antibody was simply conjugated onto *S. aureus*. Then, the engineered *S. aureus* served as a red-colored bioprobe for detecting GCA through a coagglutination test. In the presence of GCA, the bioprobes aggregated into dense red-colored eye-visible clusters, enabling the sensitive detection of GCA with a concentration of 0.05–0.10 $\mu\text{g}/\text{mL}$. This naked-eye visualization method only takes a few minutes to detect GCA and avoids the use of expensive equipment. It represents a rapid, convenient, and simple method for detecting GCA to diagnose liver diseases.



INTRODUCTION

Liver disease has brought tremendous danger to human beings, affecting the health of millions of people worldwide in the past decades. Liver diseases, such as alcoholic liver disease (ALD), nonalcoholic fatty liver disease (NAFLD), hepatitis C virus (HCV) and hepatitis B virus (HBV) infections, hepatocellular carcinoma (HCC), and cirrhosis, result in high morbidity and mortality in the world.^{1–5} For instance, over 2 billion people are being affected by HBV globally.⁶ HCC accounts for 70–90% of primary liver cancer (PLC), and more than 500,000 new HCC cases are diagnosed every year worldwide.^{7–11}

Glycocholic acid (GCA) is synthesized in the liver as cholic acid (CA) and then combined with glycine.¹² Under normal circumstances, the glycocholic acid content in the blood remains low, whether before or after a meal. Damage to liver cells or cholestasis can cause GCA metabolic disorders. As a result, the ability of liver cells to absorb GCA is reduced, which leads to an increase in GCA blood levels.^{13,14} Serum GCA concentration has been a sensitive and specific biomarker of hepatic function.^{15–21} Therefore, Serum GCA is of great significance for the clinical diagnosis of liver diseases. In addition, some studies have shown that patients with liver cirrhosis have a GCA level of about 3 to 100 times higher than healthy people.^{19,22} At present, the methods for determining

GCA mainly include enzyme-linked immunosorbent assay (ELISA),²³ gas chromatography,²⁴ high-performance liquid chromatography,^{19,25–28} and gas chromatography–mass spectrometry.²⁹ However, these methods are not suitable for clinical diagnosis because they require tedious preconditioning, expensive equipment, and well-trained analysts. Thus, they are time-consuming, limiting their applications in large-scale clinical sample analysis.

To develop a simple and effective GCA test useful in laboratory medicine, we proposed to establish a coagglutination test (Scheme 1) since it is a naked-eye visualization assay of relative technical simplicity, rapid response, low cost, and easy miniaturization. Toward this end, we first prepared a novel monoclonal antibody (mAb) of GCA. Because the Fc fragment of this anti-GCA antibody could naturally bind to protein A on a previously reported red-colored bacteria *S. aureus*,³⁰ such bindings generated an anti-GCA antibody-

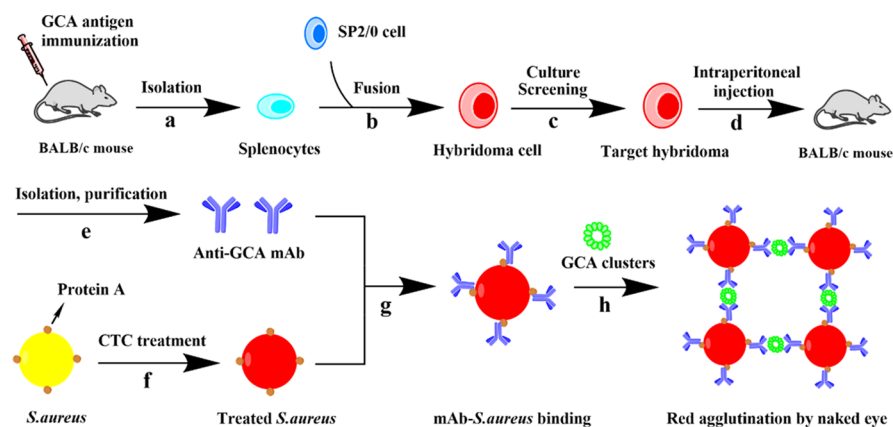
Received: August 31, 2021

Accepted: November 9, 2021

Published: November 18, 2021



Scheme 1. Schematic Illustration of GCA Bioprobe Preparation and Visually Enhanced Coagglutination Test of GCA^{a,b,c,d,e,f,g,h}



^aSplenocytes were isolated from the spleen of BALB/c mice immunized with a GCA antigen. ^bHybridoma cells were obtained through the fusion of splenocytes and SP2/0 cells. ^cThe target hybridoma cloned was acquired by further culturing and screening. ^dThe target hybridoma cloned was injected into mice to collect ascites containing antibodies by intraperitoneal injection. ^eThe anti-GCA monoclonal antibody was isolated and purified from ascites. ^f*Staphylococcus aureus* (*S. aureus*) turns red after CTC treatment. ^gA probe (mAb-*S. aureus* conjugate) is formed due to the combination of protein A on *S. aureus* and the Fc segment of the mAb. ^hWhen the probe and a sample containing GCA (probably forming a smaller cluster due to non-covalent interactions between GCA) is mixed on a glass slide, a larger red cluster is formed on the slide due to the recognition between the GCA cluster and anti-GCA, allowing us to detect the GCA by naked-eye visualization of the red spots.

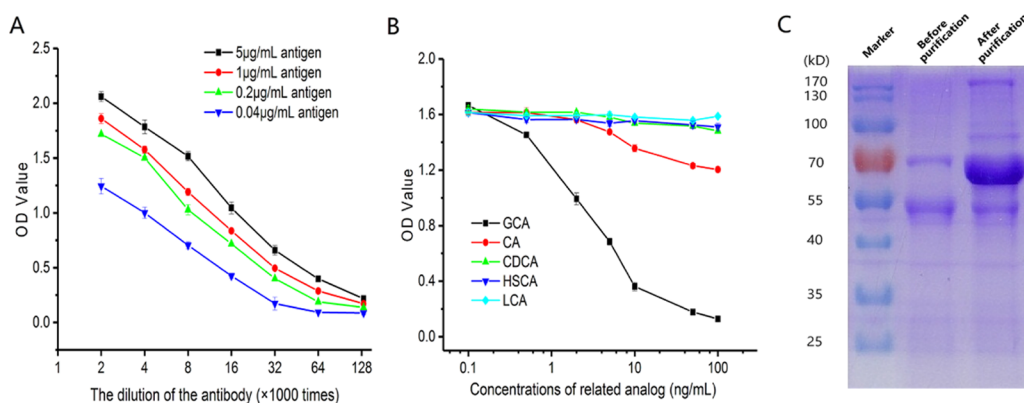


Figure 1. Characterization of the anti-GCA monoclonal antibody. (A) Affinity result of the antibody. CA: cholic acid, CDCA: chenodeoxycholic acid, HSCA: hyodesoxycholic acid, and LCA: lithocholic acid; (B) cross-reactivity analysis of the antibody by indirect competitive enzyme-linked immunosorbent assay (ic-ELISA). (C) Sodium dodecyl sulfate polyacrylamide gel electrophoresis (SDS-PAGE) of the anti-GCA monoclonal antibody before and after purification.

functionalized bacterial bioprobe (Scheme 1). We found that the addition of the bioprobes into a drop of GCA solution on a glass slide could lead to the aggregation of the bioprobes into a red spot on the slide, allowing us to rapidly and visually detect the GCA with high specificity and sensitivity.

RESULTS AND DISCUSSION

The affinity and specificity of the anti-GCA mAb were explored using indirect competitive ELISA. Briefly, as shown in Figure 1a, when the mAb samples were diluted 128,000 times, the mAb still had good affinity for the antigen. It shows that the mAb had high affinity constant with GCA. The specificity of the anti-GCA mAb was detected toward five analogs. Figure 1b shows that the CR of GCA is much higher than that of GCA analogs. With the increase of concentration, the competitive reaction becomes stronger, resulting in the decrease of OD values of GCA and indicating that the anti-GCA mAb was highly specific for GCA. The anti-GCA mAb contains light chains, heavy chains, and other proteins. Light

and heavy chains are about 25kDa and about 50–70 kDa in size, respectively. Figure 1c shows the characteristics of the anti-GCA mAb purified by caprylic acid-ammonium sulfate precipitation. The mAb samples before purification had many hetero-proteins, while the mAb samples after purification contained few hetero-proteins and retained the target protein. In addition, the color of the target protein band was deepened. Hence, the anti-GCA mAb mainly contained light (L) chains and heavy (H) chains (about 60 kDa) from SDS-PAGE, and many impure proteins were removed. As a result, the concentration of the target protein increased after purification.

Owing to the natural binding ability between protein A on the surface of *S. aureus* and the Fc fragment of mouse antibody,³¹ the red-colored bioprobes could be formed due to the binding between the anti-GCA mAb and red *S. aureus*. When GCA is present in the samples, the detection bioprobes are aggregated into dense, red-colored eye-visible clusters by antigen–antibody specific binding. When a certain number of bioprobes are aggregated, the dense red aggregates can be

observed using naked eyes due to the red color of the bioprobes, thereby semi-quantifying the GCA in the coagglutination test. When GCA is absent in the samples, the red detection bioprobe would be dispersed in the system, preventing the formation of red aggregates (Scheme 1).

S. aureus is normally pale golden yellow (Figure 2A). However, after treatment with CTC and heating, it became red

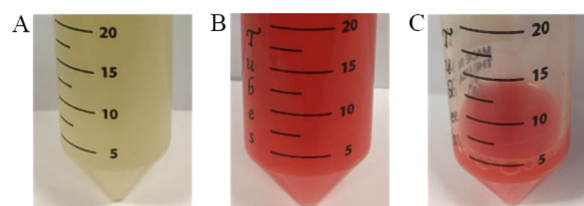


Figure 2. Photographs of the bacteria in different states. (A) Live yellow *S. aureus*. (B) CTC-transformed unculturable red *S. aureus*. (C) Bioprobes formed by binding of the anti-GCA mAb onto the red *S. aureus*.

(Figure 2). The bacteria suspension was indeed red with the naked eye (Figure 2B). After the anti-GCA mAb was bound to the red-colored bacteria through the natural binding between the Fc fragment of the mAb and protein A on the bacteria, a red bioprobe suspension was formed (Figure 2C). The color change took place because CTC reacted with the *S. aureus* to produce a red color. Also, heating the bacteria deactivated them and turned them into a dispersed state. As is shown in Figure 3A, *S. aureus* appeared well dispersed with a red fluorescent signal after heating under the fluorescence microscope, indicating the successful preparation of the red-colored bacteria. The dynamic light scattering (DLS) result confirms that the size of the probes is fairly monodisperse (Figure 3B).

When different concentrations of GCA solution from a tube (0.83, 0.42, 0.21, 0.10, and 0.05 $\mu\text{g/mL}$ and blank control) were added to the bacteria bioprobe solution on the glass slide, the detection system would accumulate into clusters through the binding of the antigen and antibody. As is shown in Figure 4, group A is the positive group (in which different concentrations of GCA were added to the bioprobes on the glass slide) and exhibited obvious red agglomerates. However, group B is the negative group (in which PBS buffer without GCA is added to the bioprobe on the glass slide) and did not

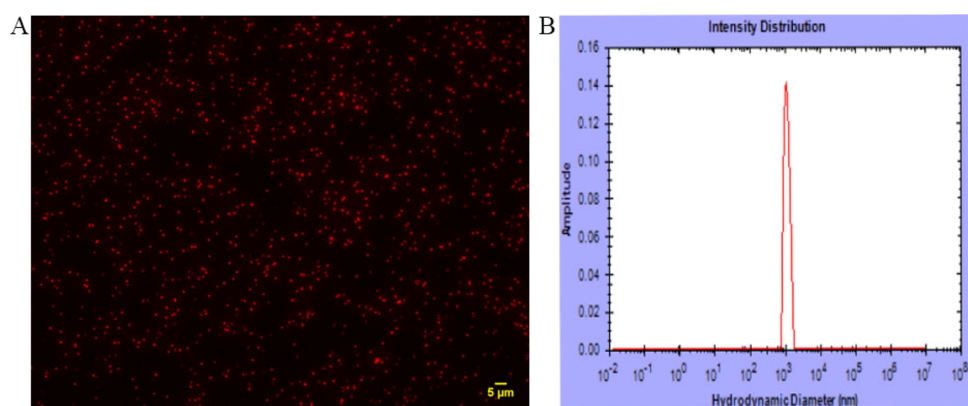
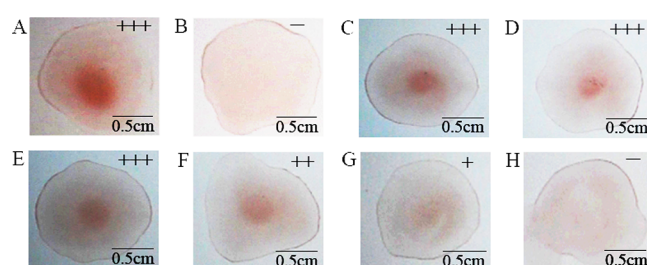


Figure 3. Characterization of the bacteria bioprobes. (A) Fluorescence image of the red *S. aureus* bioprobe. (B) DLS result of the bioprobes. These data show that the bioprobes are uniform and disperse.



+++ , condense and obvious coagglutination products;

++ , obvious and massive scattered coagglutination products;

+ , obvious but less scattered coagglutination products;

- , no coagglutination product observed

Figure 4. Coagglutination test of GCA with different concentrations by the bioprobes: (A) positive (a drop of mixture on a glass slide by coagglutination), (B) negative (there is no coagglutination in a drop of mixture on a glass slide), (C) 0.83, (D) 0.42, (E) 0.21, (F) 0.10, and (G) 0.05 $\mu\text{g/mL}$, and (H) blank. These results were recorded on a bright background with a camera.

present red agglomerates. These results confirmed that this method could detect GCA. When the GCA concentration was decreased from 0.83 to 0.1 $\mu\text{g/mL}$, the bioprobes accumulated into visible red clusters due to their specific, strong binding of GCA (Figure 4). When the GCA concentration was as low as 0.05 $\mu\text{g/mL}$, the system would not accumulate into visible clusters, indicating that 0.05 $\mu\text{g/mL}$ is the limit of detection.

Transmission electron microscopy (TEM) imaging confirmed that the bacteria bioprobes were uniform in size and well dispersed in the absence of GCA (Figure 5A). When GCA was added to the bioprobe solution, the agglutination reaction was triggered by the specific recognition between GCA and the anti-GCA mAb on the bioprobes (Figure 5B,C). These results clearly verified the mechanism of detecting GCA by the bacteria bioprobes.

To evaluate the specificity of this method for detecting GCA, cross-reactivity was evaluated by observing the red aggregates with the naked eye in the presence of GCA or its analogs. We assessed seven analogs with structures and functions close to GCA. Concentrated red aggregates were observed due to the presence of GCA (Figure 6A). However,

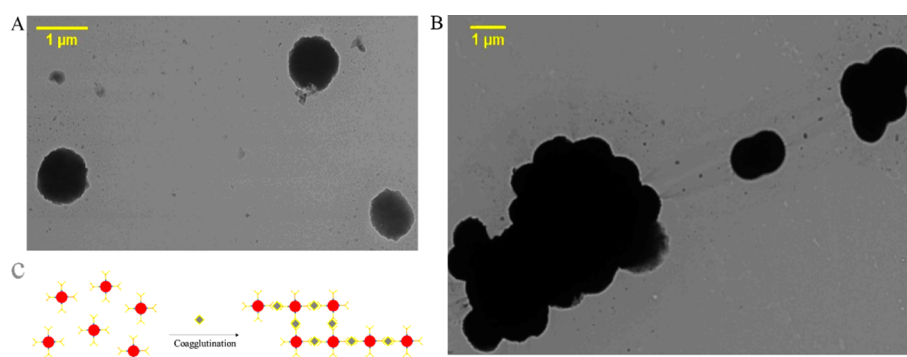


Figure 5. TEM images of bacteria bioprobes. (A) Bioprobes before the coagglutination test. (B) Bioprobes aggregated in the coagglutination test. (C) Schematic showing the coagglutination process of bioprobes due to their binding with GCA.

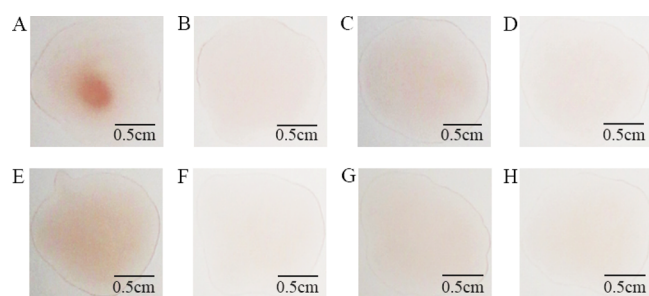


Figure 6. Specificity of the bioprobes: (A) GCA, (B) deoxycholic acid, (C) ursodesoxycholic acid, (D) glycylic ursodeoxycholic acid, (E) glycochenodeoxycholic acid, (F) taurocholic acid, (G) hyodeoxycholic acid, and (H) cholic acid. These results were recorded on a bright background with a camera.

concentrated red aggregates were almost invisible in the presence of seven analogs (Figure 6B–H). These observations indicate that the anti-GCA mAb is highly GCA-specific, enabling the coagglutination test to detect GCA with good specificity (Figure 6). Moreover, we found that our method is reproducible and stable (Figures S1 and S2). In addition, we believe that GCA tends to aggregate into clusters or even nanoparticles (Figure S3) so that antibodies could recognize different sites on them, promoting the coagglutination test to detect GCA (Scheme 1h).

CONCLUSIONS

We first developed an mAb with good affinity and specificity, the key GCA-capturing motif for the detection of GCA, a biomarker for evaluating the function of hepatocytes and the circulation function of hepatobiliary substances. We then designed a simple coagglutination detection method. In order to increase visual sensitivity, we labeled a red-colored *S. aureus* with the anti-GCA mAb to form a bacteria bioprobe. We verified that this bioprobe could capture and detect GCA by aggregation into dense red-colored aggregates visible to our naked eyes. Therefore, this method could be used to qualitatively detect GCA, potentially providing a naked-eye visualized detection method for diagnosing liver diseases.

EXPERIMENTAL SECTION

Materials and Instrument. GCA, cholic acid (CA), chenodeoxycholic acid (CDCA), hyodesoxycholic acid (HSCA), and lithocholic acid (LCA) were obtained from Aladdin Co. Ltd. Freund's complete and incomplete adjuvants were obtained from Sigma-Aldrich. Tetramethylbenzidine

(TMB) substrate solution and phosphate-buffered saline (PBS) buffer were received from Thermo Fisher Scientific Inc. The 96-well microplates and cell culture plates were obtained from Costar Inc. The mice were from Guangdong Medical Laboratory Animal Center (Guangdong, China).

Preparation of Anti-GCA mAb. The anti-GCA mAb was obtained by following previous protocols.^{32,33} Animal experiments were conducted according to the guidelines about animal ethical care of the Guangdong University of Technology. Simply, the GCA-BSA solution was mixed with Freund's adjuvant to obtain a GCA emulsion. Each BALB/c female mouse was immunized with GCA emulsion by intraperitoneal injection at two-week intervals. After the fourth immunization, the mice with high affinity for GCA were selected for a hybridoma experiment. The active SP2/0 murine myeloma cells were fused with fresh spleen cells of the mouse with polyethylene glycol 1450 (PEG 1450, sterile). After the fusion, hybridoma cells were cultured and screened by the competitive ELISA to obtain a cell strain with high specificity and sensitivity against GCA. The screened hybridoma cells were injected intraperitoneally into mice and ascites were collected 7–12 days after inoculation. Centrifugation was carried out to clarify the ascites. The octanoic acid and ammonium sulfate precipitation was used to purify the antibodies. The precipitated protein was pelleted by centrifugation, renatured by the addition of PBS, and dialyzed extensively against PBS. Finally, the mAb was collected and stored at $-20\text{ }^{\circ}\text{C}$ dialyzed.³⁴

Characterization of Anti-GCA mAb. The affinity and sensitivity of the anti-GCA mAb were characterized for binding of GCA by ELISA. The GCA antigen dissolved in carbonate buffer solution (CBS) was coated on the highly binding polystyrene solid phase in 96-well microtiter plates at $4\text{ }^{\circ}\text{C}$ overnight. Free binding sites were blocked with skim milk powder at $37\text{ }^{\circ}\text{C}$ for 1 h. After being washed with PBST, the mAb in a dilution series was incubated with the immobilized GCA at $37\text{ }^{\circ}\text{C}$ for 1 h. The plates were rinsed and aged at $37\text{ }^{\circ}\text{C}$ in the presence of the peroxidase-conjugated goat anti-mouse IgG antibody for 1 h. Unbound conjugated molecules were removed by washing with PBST. Tetramethylbenzidine (TMB) substrate solutions were added for each well. After 10 min, the reaction was terminated using H_2SO_4 (2 M) and the OD signals at 450 nm were determined.

The specificity of the anti-GCA mAb was investigated by evaluating the cross-reactivity (CR) of the analytes compared to GCA. The CR of the mAb against GCA as well as its analogs, including cholic acid (CA), chenodeoxycholic acid

(CDCA), hyodesoxycholic acid (HSCA), and lithocholic acid (LCA), was defined and calculated as follows:

$$\text{CR (\%)} = (\text{IC}_{50} \text{ of GCA} / \text{IC}_{50} \text{ of a related analog}) \times 100\%^{35}$$

Preparation of GCA-Binding Bioprobes. Red-colored *S. aureus* was prepared as reported previously.³⁰ Briefly, *S. aureus* was incubated using 5-cyano-2,3-ditoly tetrazolium chloride (CTC) and thermally treated at 65 °C for 30 min to reach an unculturable red-fluorescent state.^{36–38} The anti-GCA mAb was conjugated onto the red-colored *S. aureus* by the binding between the Fc fragment of the mAb and protein A on *S. aureus*,³⁹ producing GCA-binding bioprobes suspended in phosphate-buffered saline (PBS).

Characterization of Bioprobes. In order to study the monodispersity and homogeneity of the bioprobes, we used DLS and TEM to determine them. Since the bioprobes could fluoresce a red color, we also imaged the bioprobes by fluorescence microscopy.

Sensitivity Determination. A series of spiked GCA aqueous solutions were prepared by dilution to reach the following concentrations: 0.83, 0.42, 0.21, 0.10, and 0.05 μg/mL. A blank sample not containing GCA was also prepared. The final concentration of bioprobes was 10¹⁰ particles/mL. To detect GCA from the samples, 25 μL of the bioprobe suspension was mixed with 25 μL of the GCA samples on the glass slide. The coagglutination products could be observed with naked eyes in 5 min and verified the presence of GCA in the samples.

Specificity Demonstration. We allowed glycochenodeoxycholic acid, ursodesoxycholic acid, glycy ursodesoxycholic acid, taurocholic acid, hyodeoxycholic acid, cholic acid, and deoxycholic acid to cross-react with the bioprobes. The results were used to verify the specificity of the bioprobes in detecting GCA.

Stability, Repeatability, and Reproducibility. The stability, repeatability, and reproducibility of the bioprobes for detecting GCA were evaluated following our previous method.³⁰

■ ASSOCIATED CONTENT

SI Supporting Information

The Supporting Information is available free of charge at <https://pubs.acs.org/doi/10.1021/acsomega.1c04779>.

Characterization of repeatability, reproducibility, stability, sensitivity, and specificity and dynamic light scattering results of aggregates in solutions (PDF)

■ AUTHOR INFORMATION

Corresponding Authors

Suqing Zhao – Department of Pharmaceutical Engineering, School of Biomedical and Pharmaceutical Sciences, Guangdong University of Technology, Guangzhou 510006, China; orcid.org/0000-0002-8458-671X; Email: sqzhao@gdut.edu.cn

Chuanbin Mao – Department of Chemistry and Biochemistry, Stephenson Life Sciences Research Center, University of Oklahoma, Norman, Oklahoma 73019-5300, United States; orcid.org/0000-0002-8142-3659; Email: maophage@gmail.com

Authors

Ding Shen – Department of Pharmaceutical Engineering, School of Biomedical and Pharmaceutical Sciences,

Guangdong University of Technology, Guangzhou 510006, China; Department of Chemistry and Biochemistry, Stephenson Life Sciences Research Center, University of Oklahoma, Norman, Oklahoma 73019-5300, United States
Wei Hu – The People's Hospital of China Three Gorges University the First People's Hospital of Yichang, Yichang, Hubei 443000, China; Department of Chemistry and Biochemistry, Stephenson Life Sciences Research Center, University of Oklahoma, Norman, Oklahoma 73019-5300, United States

Complete contact information is available at: <https://pubs.acs.org/doi/10.1021/acsomega.1c04779>

Author Contributions

^{||}D.S. and W.H. have contributed equally.

Notes

The authors declare no competing financial interest.

■ ACKNOWLEDGMENTS

C.M. would like to thank the support from the Institute of Biomedical Engineering, Science and Technology of the University of Oklahoma. S.Z. would like to thank the support from the Guangzhou Science and Technology Foundation (201903010034), the Natural Resources Science Foundation of Guangdong Province (2018A030313926), the Science and Technology Foundation Key R&D Program of Guangdong Province (2019B020209009 and 2019B020218009), the R&D Program of Guangdong Province Drug Administration (2021TDZ09 and 2021YDZ06). W.H. would like to thank the support of the Natural Science Foundation of Hubei Province (2019CFB320), the Chenguang Plan (2017) of Hubei Science and Technology Association and the Yichang Science and Technology Association.

■ REFERENCES

- (1) Polasek, M.; Fuchs, B. C.; Uppal, R.; Schühle, D. T.; Alford, J. K.; Loving, G. S.; Yamada, S.; Wei, L.; Lauwers, G. Y.; Guimaraes, A. R.; Tanabe, K. K.; Caravan, P. Molecular MR imaging of liver fibrosis: A feasibility study using rat and mouse models. *J. Hepatol.* **2012**, *57*, 549–555.
- (2) Fuchs, B. C.; Wang, H.; Yang, Y.; Wei, L.; Polasek, M.; Schühle, D. T.; Lauwers, G. Y.; Parkar, A.; Sinskey, A. J.; Tanabe, K. K.; Caravan, P. Molecular MRI of collagen to diagnose and stage liver fibrosis. *J. Hepatol.* **2013**, *59*, 992–998.
- (3) Farrar, C. T.; DePeralta, D. K.; Day, H.; Rietz, T. A.; Wei, L.; Lauwers, G. Y.; Keil, B.; Subramaniam, A.; Sinskey, A. J.; Tanabe, K. K.; Fuchs, B. C.; Caravan, P. 3D molecular MR imaging of liver fibrosis and response to rapamycin therapy in a bile duct ligation rat model. *J. Hepatol.* **2015**, *63*, 689–696.
- (4) Motola, D. L.; Caravan, P.; Chung, R. T.; Fuchs, B. C. Noninvasive Biomarkers of Liver Fibrosis: Clinical Applications and Future Directions. *Curr. Pathobiol. Rep.* **2014**, *2*, 245–256.
- (5) Spengler, E. K.; Loomba, R. Recommendations for Diagnosis, Referral for Liver Biopsy, and Treatment of Nonalcoholic Fatty Liver Disease and Nonalcoholic Steatohepatitis. *Mayo Clin. Proc.* **2015**, *90*, 1233–1246.
- (6) Lok, A. S. F. Prevention of hepatitis B virus-related hepatocellular carcinoma. *Gastroenterology* **2004**, *127*, S303–S309.
- (7) Yu, M. C.; Yuan, J. M. Environmental factors and risk for hepatocellular carcinoma. *Gastroenterology* **2004**, *127*, S72–S78.
- (8) Parkin, D. M.; Bray, F.; Ferlay, J.; Pisani, P. Estimating the world cancer burden: Globocan 2000. *Int. J. Cancer* **2001**, *94*, 153–156.
- (9) Bosch, F. X.; Ribes, J.; Díaz, M.; Cléries, R. Primary liver cancer: worldwide incidence and trends. *Gastroenterology* **2004**, *127*, S5–S16.

- (10) Sherman, M. Hepatocellular carcinoma: epidemiology, risk factors, and screening. *Semin. Liver Dis.* **2005**, *25*, 143–154.
- (11) Fattovich, G.; Stroffolini, T.; Zagni, I.; Donato, F. Hepatocellular carcinoma in cirrhosis: incidence and risk factors. *Gastroenterology* **2004**, *127*, S35–S50.
- (12) Reshetnyak, V. I. Physiological and molecular biochemical mechanisms of bile formation. *World J. Gastroenterol.* **2013**, *19*, 7341–7360.
- (13) Collazos, J.; Mendarte, U.; De Miguel, J. Clinical value of the determination of fasting glycocholic acid serum levels in patients with liver diseases. A comparison with standard liver tests. *Gastroenterol. Clin. Biol.* **1993**, *17*, 79–82.
- (14) Ferraris, R.; Fiorentini, T.; Colombatti, G.; Carosso, R.; De La Pierre, M.; Eandi, M.; Ricci-Gamalerò, S. Meal stimulated response of serum bile acids levels in normal and altered bile acids enterohepatic circulation. *Boll. - Soc. Ital. Biol. Sper.* **1981**, *57*, 310–315.
- (15) Pagani, A.; Pranzo, A.; Galante, T. Determination of cholyglycine in alcoholic hepatopathies. Clinical usefulness. *Minerva Dietol. Gastroenterol.* **1985**, *31*, 25–31.
- (16) Salmi, A.; Pizzoccolo, G.; Uccelli, P.; Paterlini, A.; Moretti, R. Serum cholyglycine in the evaluation of impaired hepatic function. *Minerva Med.* **1986**, *77*, 687–691.
- (17) Pares, A.; Deulofeu, R.; Gimenez, A.; Caballeria, L.; Bruguera, M.; Caballeria, J.; Ballesta, A. M.; Rodes, J. Serum hyaluronate reflects hepatic fibrogenesis in alcoholic liver disease and is useful as a marker of fibrosis. *Hepatology* **1996**, *24*, 1399–1403.
- (18) Li, T.; Chiang, J. Y. Bile Acid signaling in liver metabolism and diseases. *J. Lipids* **2012**, *2012*, 1–9.
- (19) Li, H.; Zhao, H.; Li, Q.; Meng, D.; Li, Z. Analysis of Glycocholic Acid in Human Plasma and Urine from Hepatocellular Carcinoma Patients. *Chromatographia* **2017**, *80*, 209–215.
- (20) Collazos, J. Glycocholic Acid in Chronic Active Hepatitis and Mild Liver Diseases. *Clin. Invest.* **1993**, *72*, 36–39.
- (21) Zhang, A.; Sun, H.; Yan, G.; Han, Y.; Ye, Y.; Wang, X. J. Urinary metabolic profiling identifies a key role for glycocholic acid in human liver cancer by ultra-performance liquid-chromatography coupled with high-definition mass spectrometry. *Clin. Chim. Acta* **2013**, *418*, 86–90.
- (22) Tanggo, Y.; Fujiyama, S.; Kin, F.; Tashiro, A.; Shiraoku, H.; Akahoshi, M.; Sato, Y.; Hashiguchi, O.; Sagara, K. Clinical usefulness of serum cholyglycine determination in various liver diseases. *Gastroenterol. Jpn.* **1982**, *17*, 447–452.
- (23) Collins, D. M.; Tisch, G.; Campbell, C. B. Evaluation of enzymic and radioimmunoassay methods for measuring serum bile acids. *Pathology* **1980**, *12*, 623–629.
- (24) Karlaganis, G.; Paumgartner, G. Determination of bile acids in serum by capillary gas-liquid chromatography. *Clin. Chim. Acta* **1979**, *92*, 19–26.
- (25) Parris, N. Determination of free and conjugated bile acids ultraviolet-absorbing ion pairs by reverse-phase high-performance liquid chromatography. *Anal. Biochem.* **1979**, *100*, 260–263.
- (26) Perwaiz, S.; Tuchweber, B.; Mignault, D.; Gilat, T.; Yousef, I. M. Determination of bile acids in biological fluids by liquid chromatography-electrospray tandem mass spectrometry. *J. Lipid Res.* **2001**, *42*, 114–119.
- (27) Bloch, C. A.; Watkins, J. B. Determination of conjugated bile acids in human bile and duodenal fluid by reverse-phase high-performance liquid chromatography. *J. Lipid Res.* **1978**, *19*, 510–513.
- (28) Li, Q. F.; Zhan, Y. M.; Zhong, Y. G.; Zhang, B.; Ge, C. Q. Macromolecular Crowding Agents-Assisted Imprinted Polymers For Analysis Of Glycocholic Acid In Human Plasma And Urine. *Biomed. Chromatogr.* **2016**, *30*, 1706–1713.
- (29) BakolaChristianopoulou, M. N.; Apazidou, K. K.; Psarros, L. A new method of bile acid silylation for their GLC-MS analysis. *Appl. Organomet. Chem.* **1996**, *10*, 531–535.
- (30) Hu, W.; Zhang, Y.; Yang, H.; Yu, J.; Wei, H. Simple and rapid preparation of red fluorescence and red color *S. aureus* derived nanobiotopes for pathogen detection. *J. Microbiol. Methods* **2015**, *115*, 47–53.
- (31) Mazigi, O.; Schofield, P.; Langley, D. B.; Christ, D. Protein A superantigen: structure, engineering and molecular basis of antibody recognition. *Protein Eng., Des. Sel.* **2019**, *32*, 359–366.
- (32) Shen, D.; Zheng, J.; Cui, X. P.; Chen, Y. S.; He, Q. Y.; Lv, R.; Li, Z. X.; Zhao, S. Q. Analysis of cholyglycine acid as a biomarker for the early diagnosis of liver disease by fluorescence polarization immunoassay. *Sens. Actuators, B* **2018**, *256*, 846–852.
- (33) Huang, P.; Zhao, S.; Eremin, S. A.; Zheng, S.; Lai, D.; Chen, Y.; Guo, B. A fluorescence polarization immunoassay method for detection of the bisphenol A residue in environmental water samples based on a monoclonal antibody and 4'-(aminomethyl)fluorescein. *Anal. Methods* **2015**, *7*, 4246–4251.
- (34) Peng, J.; Meng, X.; Deng, X.; Zhu, J.; Kuang, H.; Xu, C. Development of a monoclonal antibody-based sandwich ELISA for the detection of ovalbumin in foods. *Food Agric. Immunol.* **2014**, *25*, 1–8.
- (35) Wang, Z.; Wu, X.; Liu, L.; Xu, L.; Kuang, H.; Xu, C. Rapid and sensitive detection of diclazuril in chicken samples using a gold nanoparticle-based lateral-flow strip. *Food Chem.* **2020**, *312*, 126116.
- (36) Datta, S.; Janes, M. E.; Simonson, J. G. Immunomagnetic separation and coagglutination of *Vibrio parahaemolyticus* with anti-flagellar protein monoclonal antibody. *Clin. Vaccine Immunol.* **2008**, *15*, 1541–1546.
- (37) Nafan, M. K.; Kurniasih, K.; Untari, T.; Prakoso, Y. A. Development of a coagglutination kit as a rapid test for diagnosing Newcastle disease in poultry. *Vet. World* **2020**, *13*, 1719–1724.
- (38) Wang, F. S.; Fan, J. G.; Zhang, Z.; Gao, B.; Wang, H. Y. The global burden of liver disease: the major impact of China. *Hepatology* **2014**, *60*, 2099–2108.
- (39) Xiong, L.-H.; Cui, R.; Zhang, Z.-L.; Yu, X.; Xie, Z.; Shi, Y.-B.; Pang, D.-W. Uniform Fluorescent Nanobiotopes for Pathogen Detection. *ACS Nano* **2014**, *8*, 5116–5124.